FULL PAPER

PPS www.rsc.org/pps

Catechin and hydroxybenzhydrols as models for the environmental photochemistry of tannins and lignins

Kaya Forest,[a] Peter Wan*[a] and Caroline M. Preston[b]

[a] *Department of Chemistry, University of Victoria, P.O. Box 3065, Victoria, British Columbia, Canada V8W 3V6. E-mail: pwan@uvic.ca; Fax: (250) 721-7147; Tel: (250) 721-8976*

[b] *Pacific Forestry Centre, Natural Resources Canada, 506 West Burnside Road, Victoria, British Columbia, Canada V8Z 1M5; Fax: (250) 363-0775; Tel: (250) 363-0720*

Received 13th February 2004, Accepted 22nd March 2004
First published as an Advance Article on the web 2nd April 2004

The photochemistry of several model plant-derived compounds has been studied in aqueous solution. In particular, the reactions of catechin as a model tannin and methoxy-substituted hydroxybenzhydrols as model lignin functionalities were investigated. Tannins and lignins constitute a significant portion of the humic substances in aquatic systems, which are themselves the main component of dissolved organic matter thought to be responsible for the absorption and attenuation of light in these environments. Catechin (**1**) was found to undergo a reversible photoisomerization reaction to give epicatechin (**2**). Such a reaction is an explicit example of a photon absorbing process that enables catechin (**1**) and its derivatives to act as natural sunscreens by attenuating light energy through non-destructive reactions. The methoxy-substituted hydroxybenzhydrols were found to undergo photosolvolysis reactions *via* efficient generation of quinone methide intermediates. The intermediate quinone methides were observed to be longer lived, and thus more stable, than previously studied hydroxybenzhydrol derivatives. The *meta*-hydroxybenzhydrol isomer (**5**) was found to undergo additional chemistry leading to the production of a ring-closed fluorene from the quinone methide intermediate.

Introduction

With its ability to absorb strongly in the visible and UV regions of the solar spectrum, dissolved organic matter (DOM) from both autochthonous and allochthonous sources within an ecosystem can attenuate solar radiation through absorption and scattering processes and consequently act as a natural sunscreen.[1] Humic substances, the dominant component of DOM, are known to be among the most important natural sunlight-absorbing components of soil surfaces and they constitute half of the organic and nearly all of the coloured matter in most aquatic systems.[2,3] Studies of light-induced changes on the spectral properties of natural organic matter have shown that both isolated humic substances,[2] and total coloured DOM are bleached by exposure to visible and UV light,[4–8] and that absorption of solar radiation produces electronically excited molecules capable of participating in a variety of photosensitization reactions.[3,9] However, few mechanistic details of their direct photochemistry are known.[10,11]

Dissolved humic substances in river, lake and coastal ecosystems are derived from plant residues that have been modified by chemical and biological processes.[12,13] Because their complex and irregular structures make them resistant to biological degradation, photochemical processes are important not only as a UV screen, but also as a significant mechanism for release of CO_2 to the atmosphere and for production of smaller molecules that can be more readily utilized by microrganisms.[4–8] Tannins and lignins constitute a significant portion of plant litter[14–18] and are major components of DOM and humic substances.[2,7,19,20] They are the most likely source for the colour of DOM, and hence represent the aromatic and conjugated chromophores involved in photoprocesses.

Despite the importance of photochemical processes in aquatic ecosystems, there have been few studies of structural changes to DOM and humic substances upon irradation,[2,7,8] and as noted previously, little detailed investigation of specific photochemical processes. Photochemical studies of model tannins such as catechin (**1**) have attempted to elucidate their apparent antioxidant abilities,[21–25] but few studies have been done to characterize their photochemical reactions in an aquatic environment. Prior work in our laboratory and others has shown that hydroxybenzyl alcohols and their derivatives react photochemically to generate quinone methide intermediates.[26–29] These compounds are structurally related to lignin compounds, particularly when they contain both methoxy and hydroxy substituents, including *p*-quinone methides which are formed as important intermediates in the polymerization of precursors in lignin synthesis.[29]

Given that these types of compounds comprise a significant portion of the dissolved organic matter responsible for light attenuation in aquatic systems, it is appropriate to investigate the general photochemistry of model tannins and lignins to elucidate the potential mechanisms of this sunscreening ability. Of interest in this work is the reactivity of possible photogenerated quinone methides in an environmental setting to provide a context for the claims that humic substances, such as those derived from tannins and lignins, act as light-absorbing sunscreens in aquatic environments. Therefore, the purpose of this study is to attempt to characterize and describe photochemical reactions of humic material using model tannins (**1**–**3**) and compounds representative of lignin functionalities (**4**–**9**).

Results and discussion

Photoisomerism of catechins

Photolysis of the (−)-*cis* isomer, epicatechin (**2**), in 1:1 CH_3CN–H_2O at 254 nm gave conversion to the (−)-*trans* isomer, catechin (**1**), as determined by their distinctive ^{1}H NMR spectra and optical rotation [eqn. (1)]. The specific rotation of a solution of (−)-**2** changed from [α] = −50° to [α] = −32° after photolysis (≈50% conversion), suggesting that the photoisomer formed was (−)-**1** ([α] = −16°)[30] as opposed to the (+)-enantiomer ([α] = +16°)[30] which would have resulted in a significantly less negative specific rotation of the photolysis mixture. Small amounts of what were likely oxidative side products[31] that imparted a yellow colour to the solution were also generated but were produced in trace yields not isolable for subsequent characterization. Since **1** and **2** are closely related

DOI: 10.1039/b402241f

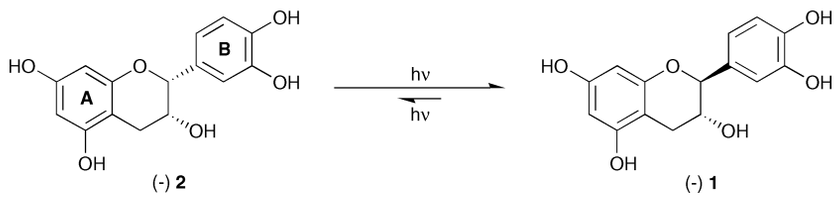

(-) **2** (-) **1** (1)

isomers they were not separable using conventional silica gel chromatography[32] and thus conversion was measured by ^{1}H NMR integration of distinctive proton signals. As shown in Fig. 1, extended photolysis of **2** resulted in the formation of **1** with a rapid increase in conversion during the initial 3 minutes of irradiation which subsequently increased more slowly and leveled off after 8 minutes at a maximum conversion of ≈90%.

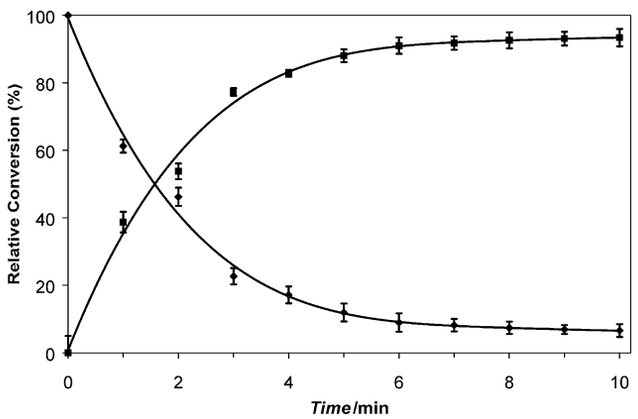

Fig. 1 Conversion of **2** (◆) to **1** (■) on photolysis at 254 nm in aqueous acetonitrile at various irradiation times.

Photolysis of (±)-**1** under similar conditions showed the reverse isomerization conversion to **2**, although conversion never exceeded ≈5%. The absolute stereochemistry could not be determined at such low conversions where the error in the specific rotation measurements were of the same magnitude as that due to any change in stereochemistry. Side reactions were detected at photolysis times longer than 5 minutes, although they did not occur in sufficient quantity to allow the isolation of any products. Photolysis of the catechin tetramethyl ether derivative (**3**) in 1 : 1 CH_3CN–H_2O at similar times also showed conversion of the *trans* isomer to the *cis* isomer in a comparable ≈5% yield.

To probe the ability of ambient light in an aquatic environment to initiate the observed bond cleavage and subsequent isomerization reaction, **2** was irradiated under similar conditions at 300 nm. Conversion of **2** to **1** was found to reach a maximum of ≈80% after 10 minutes of photolysis in 1 : 1 CH_3CN–H_2O compared to 90% at 254 nm, indicating that the described reactions can occur under natural light conditions in aquatic environments.

Photolysis of 4–9

Photolysis of the methoxy-substituted hydroxybenzhydrols **4**, **5**, and **6** in 1 : 1 CH_3OH–H_2O for 5 minutes at 254 nm under inert atmosphere gave the corresponding methyl ethers in approximately 37, 21, and 4% yield, respectively, as determined by ^{1}H NMR integration (error ±5%). Photolysis of the analogous hydroxybenzyl alcohols **7**, **8**, and **9** also gave the corresponding methyl ethers in 29, 4, and 2% yield, respectively, indicating that the presence of a benzyl phenyl group enhances the yield of transient formation and subsequent photosolvolysis product formation. At conversions of less than 20%, the corresponding methyl ethers were the only significant products. At extended photolysis times, however, small amounts of the corresponding benzylphenols and aldehydes were also isolated. Previous work[27] has shown that benzylphenols are the product of secondary photolysis of the photogenerated methyl ether of the starting hydroxybenzhydrol. Thus, the same mechanism is presumed to occur with the compounds under study which involves initial homolytic cleavage of the benzyl C–OCH_3 bond followed by disproportionation of the radical pair to yield the corresponding benzylphenol and formaldehyde. Extended photolysis of **5**, for example, resulted in the formation of methyl ether **10** which increased rapidly during the initial 15 minutes of irradiation, then subsequently rose more slowly and

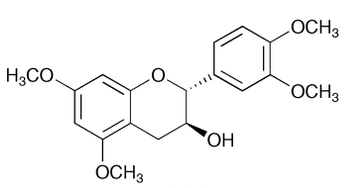

(+) **3**

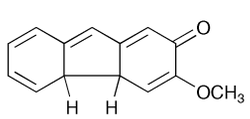

16

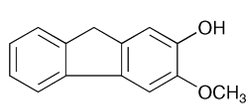

17

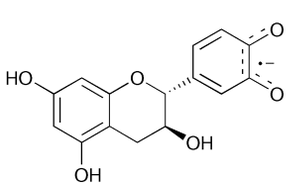

18

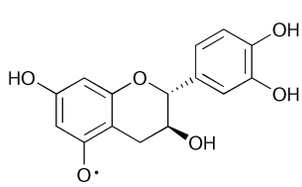

19

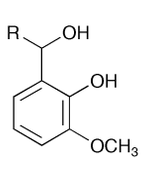

4 R = Ph
7 R = H

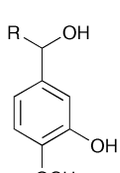

5 R = Ph
8 R = H

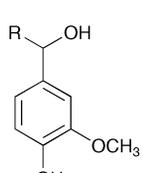

6 R = Ph
9 R = H

leveled off after 40 minutes (Fig. 2). The yield of benzylphenol **11** also followed a similar trend although it rose less rapidly and to a lower final yield at photolysis times employed. At these photolysis times, **5** had reacted to **10** in 51% yield, **11** in 19% yield, and benzaldehyde **12** in approximately 5% yield [eqn. (2)]. Proposed condensation product **13** never achieved yields greater than 1% at irradiation times studied.

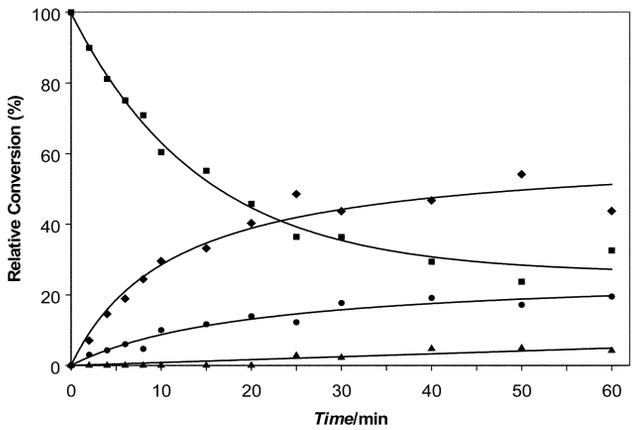

Fig. 2 Photosolvolysis conversion of **5** (■) to **10** (◆), **11** (●), and **12** (▲) in 1 : 1 CH_3OH–H_2O as a function of photolysis time.

To ascertain whether photolysis leading to the methyl ethers was the result of a carbocation or quinone methide intermediate, the *ortho*-hydroxybenzhydrol **4** was photolysed in the presence of ethyl vinyl ether. The result was a racemic mixture of regioselective chroman-like products (**14**) isolated in relatively high yield (≈75%). The *ortho*-hydroxybenzyl alcohol **7** was also found to generate the corresponding racemic chroman products (**15**) in a similar yield consistent with a [4+2] Diels–Alder type reaction of an electron poor quinone methide with an electron rich dienophile [eqn. (3)].[33,34] The photolysis reactions of the *ortho*, *meta*, and *para* isomers of the hydroxybenzhydrols and hydroxybenzyl alcohols are thus proposed to proceed through quinone methide intermediates.

Photosolvolysis was also used to determine the quantum yield of product formation (Φ_p) and by extension the quantum yield of formation of the quinone methide intermediate (Φ_{QM}) (Table 1). The product quantum yields were determined from conversion of the compound under investigation relative to the conversion of 2-hydroxybenzhydrol ($\Phi_p = 0.46 \pm 0.03$)[27] using

Table 1 Quantum yields (Φ_p) of respective methyl ether formation from irradiation in 1 : 1 CH_3OH–H_2O

Compound[a]	Φ_p	Compound	Φ_p
7	0.31 ± 0.03	**4**	0.55 ± 0.04
8	0.04 ± 0.01	**5**	0.43 ± 0.08
9	0.01 ± 0.01	**6**	0.07 ± 0.02
		20	0.38 ± 0.05

[a] Using Φ_p for photosolvolysis of 2-hydroxybenzhydrol ($\Phi_p = 0.46 \pm 0.03$)[27] as a secondary standard. Each value is the result of at least three independent trials.

^{1}H NMR integration. While the quantum yields of quinone methide formation can not be measured directly, they can be estimated from the Φ_p for photosolvolysis by the fraction of photogenerated quinone methide that leads to the methyl ether product. The nucleophilicity of water with respect to similar compounds has been shown to be about 0.8 times that of methanol in 1 : 1 CH_3OH–H_2O[27] and thus the Φ_{QM} can be estimated by applying this factor to the corresponding Φ_p.

Photolysis of **5** in aqueous acetonitrile resulted in the formation of several unique products. One isolated compound with a large molecular weight and a ^{1}H NMR similar to the starting hydroxybenzhydrol was identified as dimer **13**. A second compound had an *m*/*z* ratio (M^+) of 212 and a non-aromatic ^{1}H NMR spectrum with several methylene but no aromatic proton signals. A third fraction had an *m*/*z* ratio (M^+) of 212 and an aromatic ^{1}H NMR spectrum with two methylene protons. Due to the low yields of these two photoproducts, their separation and quality of the resulting ^{1}H NMRs were only sufficient to suggest the presence of functional groups and relative proton position, rather than make unambiguous structural assignments. However, along with laser flash photolysis data there was sufficient evidence to suggest the second compound was a conjugated non-aromatic species such as **16** and the third compound was the ring-closed substituted fluorene **17**. On sitting over several days or after gentle heating, the proposed **16** was found to convert to **17** suggesting that the conjugated **16** is a moderately stable intermediate in the mechanism of the generation of the more stable aromatic **17**.

Fluorescence measurements

The fluorescence quantum yield (Φ_f) and lifetime (τ_f) for **1**–**9** were determined in neat CH_3CN (Tables 2 and 3).[27,35] To better

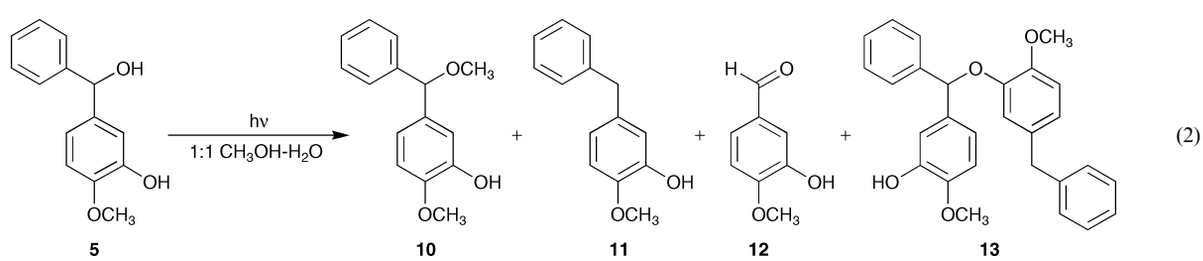

(2)

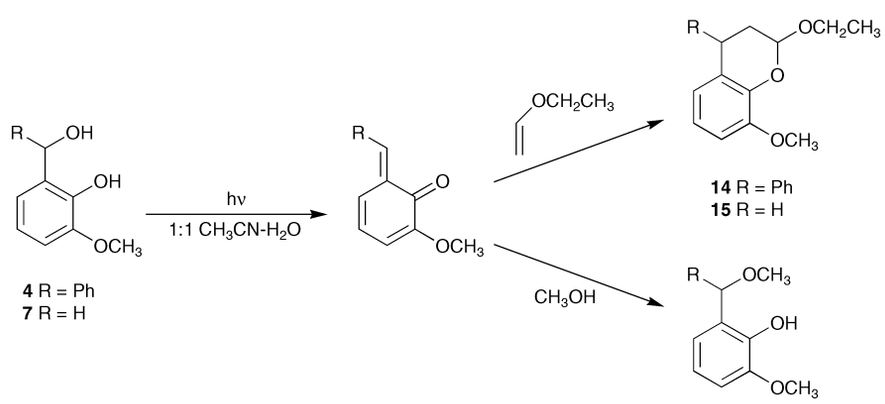

(3)

Table 2 Fluorescence quantum yields (Φ_f) and lifetimes (τ_f) for catechin system in neat CH_3CN

Compound[a]	Φ_f[b]	τ_f (ns)
1	0.15 ± 0.003	2.12
2	0.16 ± 0.01	2.07
3	0.12 ± 0.01	1.87

[a] λ_{exc} = excitation wavelength = 279 nm, λ_{em} = monitored emission wavelength = 308 nm. [b] Measured using 2-aminopyridine in 0.05 M H_2SO_4 (Φ_f = 0.60 ± 0.05)[35] and 2-hydroxybenzhydrol (Φ_f = 0.13 ± 0.01)[27] as standards. Each value is the result of at least three independent trials. Chi² values always <0.1.

understand the reactivity of **1** by trying to identify the chromophore responsible for absorption of irradiation and the observed isomerization chemistry, fluorescence quenching studies of resorcinol and catechol were performed to model the A and B rings, respectively. The fluorescence emission spectrum of **1** red-shifted from λ_{max} = 307 to 311 nm on addition of water followed by a subsequent decrease in fluorescence signal at greater water concentrations. The emission spectrum of resorcinol also red-shifted several nanometers on addition of 20% water (from λ_{max} = 298 to 301 nm), however, no significant quenching of the signal was apparent until the water content reached 100% where only moderate quenching was observed. The emission spectrum of catechol was found to red-shift several nanometers on addition of 20% water (from λ_{max} = 305 to 309 nm). Higher water concentrations resulted in greater quenching of the fluorescence signal. The similarity in the effect of water on the fluorescence of catechol and **1** suggests that it is likely the catechol-like B ring that acts as the chromophore absorbing the irradiation leading to the observed chemistry.

Lifetimes of reactive intermediates

The laser flash photolysis (LFP) of **1** in aqueous acetonitrile gave bands at λ = 370 and 490 nm consistent with previous studies in basic solution irradiated at 308 nm which identified these signals as belonging to catechol-like (**18**) and resorcinol-like (**19**) radical species, respectively.[36,37] In these studies, no corresponding signals were observed in neutral solution when irradiated at 308 nm. A third signal was apparent at λ = 310 nm in our LFP studies but was complicated by one growth and at least one decay component and was thus not assigned. The band at 370 nm had a moderate ΔOD which consisted of a short single exponential decay component with a lifetime of $\tau \approx 0.30$ ms and a longer component that did not decay within the lifetime of the laser system (>2 ms). The signal at 490 nm was weak but gave a good single exponential decay fit with a lifetime of τ = 8 μs. These results correspond with the qualitative description in previous studies where the catechol-like radical **18** at ≈380 nm was observed to be long lived and the resorcinol-like radical **19** at ≈495 nm was found to be short lived. Based on rate constant data generated by pulse-radiolysis studies, Jovanovic *et al.*[38] proposed that **19** decayed to **18** through both inter- and intramolecular electron transfer mechanisms. However, given that there was no observed growth of the catechol-like radical (**18**) with a lifetime of ≈8 μs corresponding to the decay of **19**, a lifetime readily resolved by our laser system, it can be concluded that **19** does not decay to **18** under our experimental conditions and in accordance with Cren-Olivé *et al.*[37]

Photolysis of the *ortho*-hydroxybenzhydrol **4** in aqueous acetonitrile resulted in the generation of absorption bands at λ = 348 and 485 nm attributed to an intermediate species with a lifetime of τ = 23 s. Irradiation in neat acetonitrile also resulted in the formation of the same transient with a longer lifetime (τ = 150 min) indicting that the intermediate can be generated in the absence of water. Additional experiments with this isomer were difficult to complete as the compound was found to yellow readily on exposure to ambient light with the resulting compound having limited solubility in most solvents. This was thought to be due to the efficient formation of the quinone methide intermediate and subsequent reaction with starting material in the solid state to give insoluble polymers.

Irradiation of the *para*-hydroxybenzhydrol **6** in aqueous acetonitrile resulted in the formation of an absorption band at λ = 382 nm attributed to an intermediate species with a lifetime of τ = 110 min. No transient was observed on photolysis in neat CH_3CN although photolysis in 5% water resulted in formation of the transient with a lifetime of τ = 170 min. Photolysis of **6** in increasing amounts of water resulted in a corresponding decrease in transient decay rate above 30 mol L^{-1} water (Fig. 3). In aqueous solution below 30 mol L^{-1} water, k_{obs} of the transient was found to be independent of water concentration, except that small amounts of water were required to generate the transient. The lifetime of the transient from photolysis of **6** was also measured in neat water at a variety of pH values. A plot of log k_{obs} *versus* pH gave a slope of −1.0 in solutions below pH 4 and a slope of +1.0 in solutions above pH 10 indicating that the transient is quenchable by both H^+ and OH^- *via* general acid and base catalyzed mechanisms (Fig. 4). The rate constants for **6** were thus calculated to be $k_{H^+} = 8.2 \times 10^2$ M^{-1} s^{-1} and $k_{OH^-} = 1.7 \times 10^3$ M^{-1} s^{-1}.

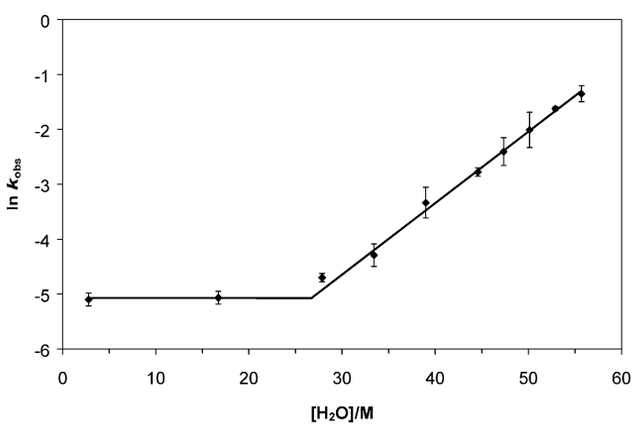

Fig. 3 Effect of increased water content on the observed rate constant for **6** ([H_2O] > 30 M: ln k_{obs} = 0.130[H_2O] − 8.552; R^2 = 0.995).

Table 3 Fluorescence quantum yields (Φ_f) and lifetimes (τ_f) for methoxy-substituted hydroxybenzyl alcohol and hydroxybenzhydrol systems and derivatives in neat CH_3CN

Compound[a]	Φ_f[b]	τ_f (ns)	Compound[c]	Φ_f[b]	τ_f (ns)
7	0.16 ± 0.004	2.24	**4**	0.21 ± 0.02	1.64
8	0.21 ± 0.001	2.53	**5**	0.25 ± 0.01	2.71
9	0.20 ± 0.002	2.50	**6**	0.22 ± 0.001	2.42
			20	0.19 ± 0.002	2.05
			11	0.32 ± 0.005	2.72

[a] λ_{exc} = excitation wavelength = 279 nm, λ_{em} = monitored emission wavelength = 308 nm. [b] Measured using 2-aminopyridine in 0.05 M H_2SO_4 (Φ_f = 0.60 ± 0.05)[35] and 2-hydroxybenzhydrol (Φ_f = 0.13 ± 0.01)[27] as standards. Each value is the result of at least three independent trials. Chi² values always <0.1. [c] λ_{exc} = excitation wavelength = 280 nm, λ_{em} = monitored emission wavelength = 308 nm.

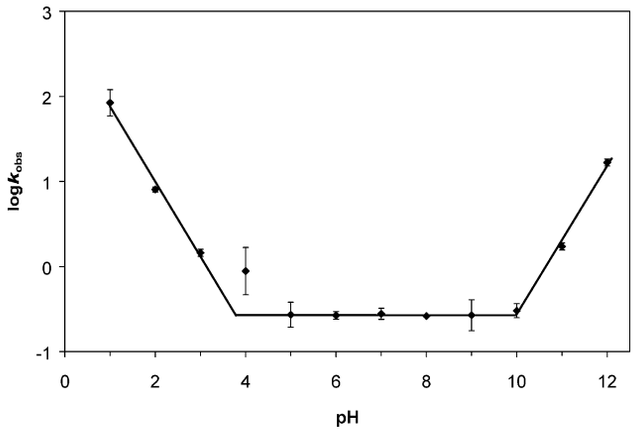

Fig. 4 Effect of pH on transient decay rate for **6**. The quoted pH is of the aqueous fraction prior to addition of acetonitrile (pH < 3: slope = −1.0, $k_{H^+} = 8.2 \times 10^2$ M^{-1} s^{-1}; pH > 10: slope = +1.0, $k_{OH^-} = 1.7 \times 10^3$ M^{-1} s^{-1}).

Using LFP, irradiation of **5** in aqueous acetonitrile gave one strong band at λ = 420 nm, consisting of a decay that could be fit with two single exponential decays (τ = 0.8 and 90 μs) and one less intense band at λ = 640 nm, consisting of one single exponential decay (τ = 80 μs) (Fig. 5). Due to the similarity in lifetime of the longer 420 nm component and the 640 nm decay, these signals are believed to arise from the same transient species. In addition, the growth of the band at 640 nm (τ = 0.5 μs) was found to have a lifetime similar to the decay of the shorter component of the 420 nm band, suggesting that the transient corresponding to the 640 nm band arises from the decay of the transient corresponding to the shorter 420 nm component. No signals were observed in neat acetonitrile, although photolysis in aqueous methanol gave a similarly shaped spectrum with the transients having shorter lifetimes (τ = 0.1 μs and 11 μs at 420 nm, and 13 μs at 640 nm), corresponding to increased reactivity of the short 420 nm intermediate with the more nucleophilic methanol.

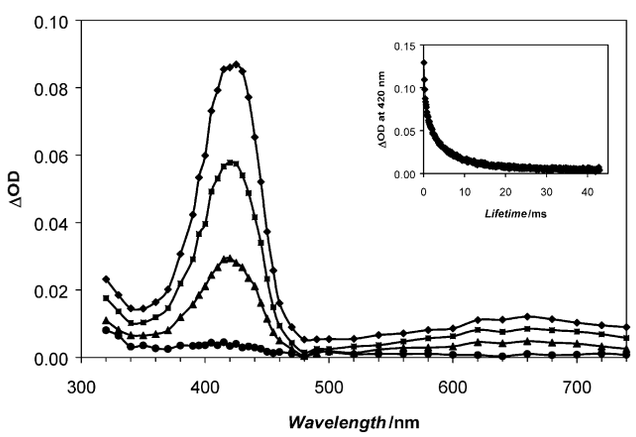

Fig. 5 Decay of transient generated from the photolysis of **5** in 1 : 1 CH_3CN–H_2O. Top to bottom: 9.5, 20, 57, and 400 μs after laser pulse (inset: transient decay taken at 5 ns intervals at λ_{max} = 420 nm, τ = 0.8 and 90 μs).

The decay of the transients for **5** were measured at a variety of pH values. At intermediate pH, the rate constants of the two transients were essentially unchanged. However, at both high and low pH the signal at 420 nm approached a single first order decay with a lifetime of τ = 0.6 μs in acidic solution (pH < 3) and τ = 11 μs in basic solution (pH > 10). The transient at 640 nm had a lifetime of τ = 0.4 μs in acidic solution (pH < 3) and τ = 12 μs in basic solution (pH > 10), corresponding to the lifetimes observed at the same pH for the 420 nm transient signal. Significant quenching of the 420 and 640 nm bands was also observed upon addition of ethanolamine (up to 0.5 M) as quencher. In the presence of ethanolamine, the signal at 420 nm also approached a single exponential decay with the rates of transient decay for both the 420 and 640 nm signals increasing to the same extent with increasing ethanolamine concentration again suggesting that the signals being quenched at 420 and 640 nm belong to the same transient. The lack of resolution of the short component of the 420 nm transient in both pH and quenching studies can be attributed to it being readily quenched by both H^+ and OH^- and by a strong nucleophile, respectively, resulting in a shortened lifetime not detectable using the laser system employed.

The longer lived signals associated with a second transient for **5** were unexpected. To determine whether the phenyl, phenol and benzyl alcohol moieties were required for formation of this transient, the photochemistry of benzyl alcohol **8**, dimethoxybenzhydrol **20** and diphenyl **11** were examined. The LFP of **8** showed a weak signal at λ = 400 nm with a lifetime of $\tau \approx 0.5$ μs but no signal at longer wavelengths corresponding to another transient. The LFP of **20** gave one strong, broad band centered at λ = 460 nm, consisting of a single exponential decay with a lifetime of τ = 0.78 μs corresponding to a carbocation intermediate that was quenchable by nucleophiles to yield photosolvolysis products, but no signal at longer wavelengths corresponding to that observed for **5** was apparent. The LFP of **11** gave one weak, broad band centered at λ = 480 nm which did not decay within the lifetime of the laser system (>2 ms), with no additional signal corresponding to that observed for **5**. It can thus be concluded that the phenyl, phenol and benzyl alcohol moieties of **5** were all required to generate the additional transient. Since **4** and **6** gave no corresponding signals, it can be inferred that a *meta* substituted hydroxy group is also required.

Mechanisms of reaction

Previous thermal studies of the isomerization of **1** and **2** postulated a quinone methide intermediate.[21,39–41] Subsequent work has suggested that epimerization can occur *via* photochemical methods, although no direct evidence for the identity of the intermediate was observed.[42,43] Investigations of the catechin system show efficient isomerization of the naturally produced (−)-*cis* isomer (**2**) to the (−)-*trans* isomer (**1**) with a photostationary state of ≈90% in favour of the less sterically hindered *trans* isomer. As a result, isomerization constitutes the dominant photochemical reaction that occurs upon photolysis of **1** and **2** under the experimental conditions employed. LFP studies also confirm the presence of two intermediates identified as catechol and resorcinol-like radicals (**18** and **19**, respectively) not previously found to be generated in neutral solution.[37]

The isomerization reaction can proceed *via* one of several mechanisms involving cleavage of the pyran O–C bond (Scheme 1). The tethered nature of the ring-opened intermediate, whether formed homolytically or heterolytically, results in re-closing of the pyran ring that is sufficiently slow to allow bond rotation to give the observed isomerization but too fast to allow trapping by nucleophiles such as methanol and radical trap solvents such as 2-propanol or to be readily observed by nanosecond LFP. The inability to isolate a ring-opened compound was unexpected given that thermal pyran ring-opening reactions using fairly mild conditions have been shown to result in the isolation in numerous ring-opened species.[41] As a consequence of the complexity seen in the LFP spectra and the limitations of resolution of the system, neither a homolytic mechanism leading to a biradical intermediate or a heterolytic mechanism leading to either a zwitterionic or quinone methide intermediate can be eliminated as possible reaction mechanisms resulting in the observed photoisomerization reaction. However, given that the tetramethyl ether derivative (**3**) undergoes a similar photoisomerization reaction yet is not capable of proceeding through a quinone methide intermediate, reaction

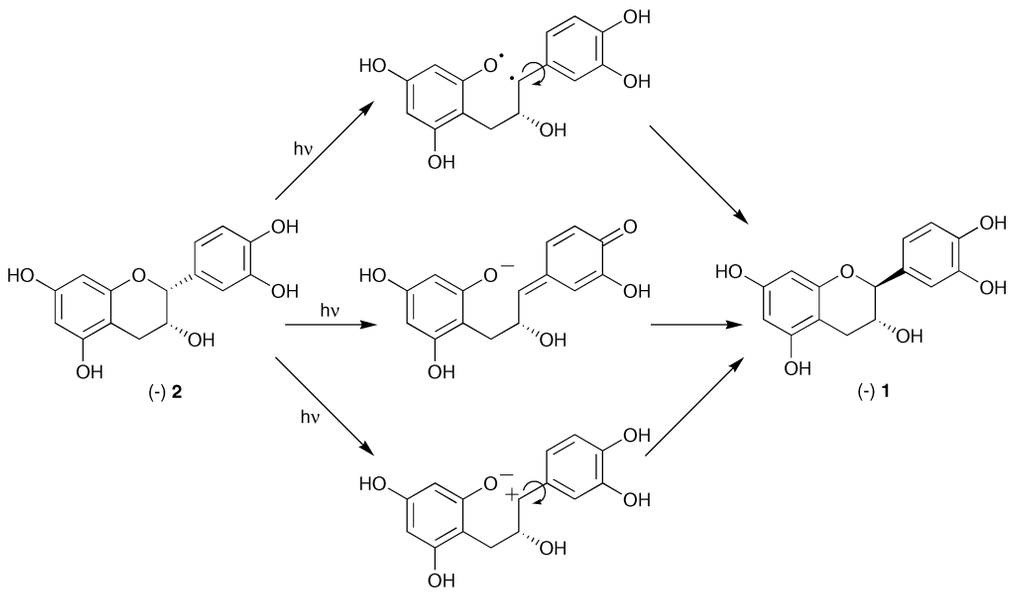

Scheme 1

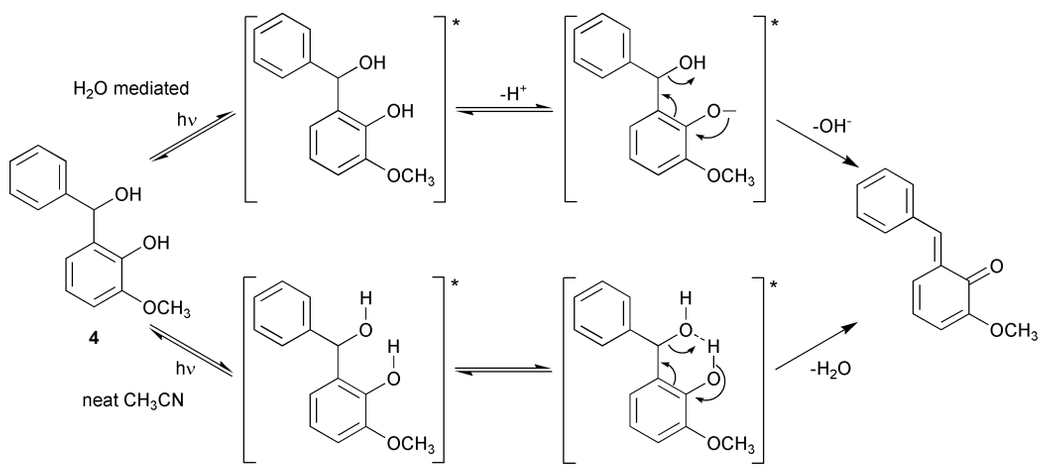

Scheme 2

through the biradical or zwitterionic intermediate may be the more likely mechanism.

The hydroxybenzhydrol system gave results consistent with previous work in our group and others for related systems.[26–28] *Ortho*, *meta* and *para* isomers of methoxy-substituted hydroxybenzyl alcohols (**7**, **8**, and **9**) and hydroxybenzhydrols (**4**, **5**, and **6**) are reactive on photolysis in aqueous methanol to give the corresponding benzyl methyl ethers in yields that followed the anticipated *ortho* > *meta* ⋙ *para*[44] pattern of reactivity. While the results of many of the experiments may be consistent with the formation of cationic intermediates, the long transient lifetimes are inconsistent with short lifetimes of similar diphenyl methyl cations.[45,46] UV-Vis and LFP studies showed that both the relative quantum yields of transient formation and the transient decay rate constant increased with the addition of water corresponding to a decrease in the fluorescence signal. These transients can be quenched both by electrophiles such as H^+, and nucleophiles such as alcohol, ethanolamine and OH^-. Such results are consistent with the formation of quinone methide intermediates. The proposed mechanism for photolysis of **4**, **5**, and **6** (and for the corresponding benzyl alcohols **7**, **8**, and **9**) in aqueous solution is water assisted adiabatic deprotonation of the excited phenol to give the singlet excited phenolate which subsequently dehydroxylates to yield the corresponding quinone methide (Scheme 2).

Unlike the *meta* and *para* isomers, photolysis of the *ortho*-hydroxybenzhydrol (**4**) in neat acetonitrile gave an observable quinone methide intermediate although in a lower yield and with a longer lifetime than in aqueous acetonitrile suggesting a second reaction mechanism in the absence of water. The location of the phenol substituent *ortho* to the benzyl alcohol group likely gives rise to significant hydrogen bonding between the two. Crystallographic analysis of 2-hydroxybenzhydrol[47] has shown that the two aromatic rings lie almost perpendicular to one another and that there is significant intramolecular hydrogen bonding between the phenoxyl proton and the benzylic oxygen. The addition of a *meta*-methoxy group in the compound under study should not affect this interaction, and it can be assumed that the three dimensional structure of **4** is very similar. Due to the presence of such extensive hydrogen bonding, a concerted mechanism for **4** could be envisioned whereby deprotonation of the phenolic group and loss of the hydrogen bonded benzylic hydroxy group generates the quinone methide *via* an intramolecular proton transfer mechanism (Scheme 2).

Many of the results for the short lived component of the 420 nm transient of **5** are consistent with results for similar *meta*-quinone methide intermediate systems. While the λ_{max} and shape of the 420 nm band observed in the LFP spectrum of **5** corresponds to diarylmethyl cations reported by McClelland *et al.* for similar substituted benzhydrols,[46] the lifetime of ≈1 μs observed for the short component is too long to be the corresponding phenylmethyl cation. Since a deprotonated hydroxy group is electron donating in the *meta* position compared to the protonated hydroxy group which is electron withdrawing in the *meta* position,[48] the ≈1 μs lifetime is significantly longer than would be predicted from a simple cation description of the

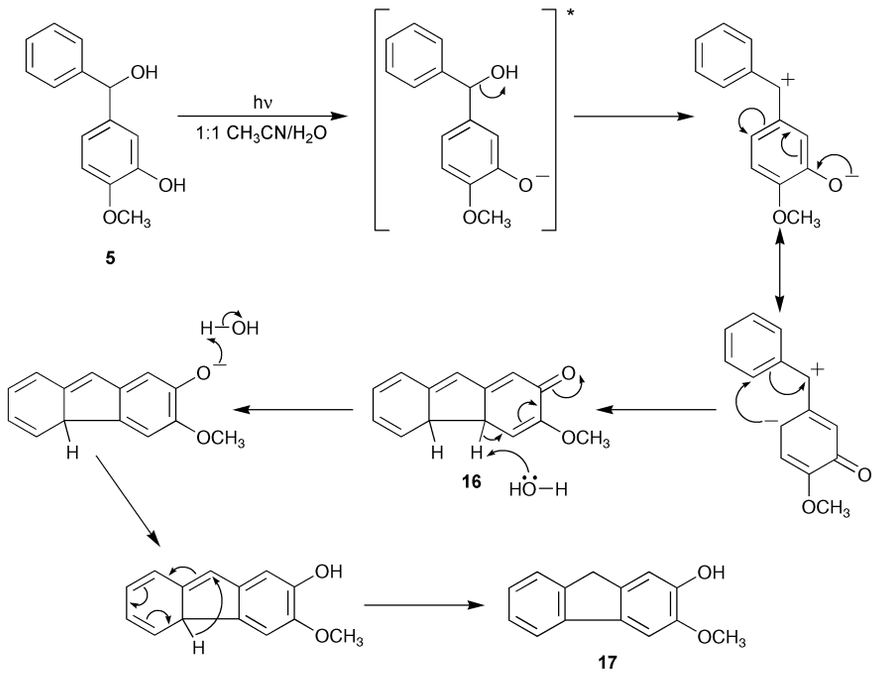

Scheme 3

transient (<0.5 μs). The transient associated with the short lived component of the 420 nm signal can therefore be assigned to the zwitterionic *meta*-quinone methide, which follows the mechanism described for water assisted quinone methide formation.

Interestingly, LFP studies of **5** indicated the presence of an intermediate in addition to the anticipated quinone methide. The long lived component of the 420 nm band and the 640 nm band had similar lifetimes and were identified as belonging to the same transient. In addition, the decay of the quinone methide at 420 nm had a similar lifetime to the growth of the signal at 640 nm, suggesting the subsequent reaction of the quinone methide to generate the transient observed. LFP studies on functional group analogues **8**, **20** and **11** determined that the phenyl, phenol and benzyl alcohol functional groups were required for the generation of this additional transient. Product studies in aqueous acetonitrile allowed the isolation of trace amounts of ring-closed products **17** and the proposed **16**. The presence of these photoproducts suggests that the quinone methide subsequently reacts through a ring-closing mechanism to generate a substituted fluorene **16** (Scheme 3). The proposed **17** was found to thermally convert to **16** further supporting the proposed mechanism.

The dimethoxy-substituted benzhydrol analogue (**20**) was subjected to photosolvolysis experiments despite previous studies of mono-substituted methoxybenzhydrol analogues which reported no reaction for similar experiments.[27] In contrast, **20** was found to undergo efficient photosolvolysis in methanol with a quantum yield ($\Phi_p = 0.38$) close to that of the corresponding *meta*-hydroxybenzhydrol **5** ($\Phi_p = 0.43$). As a result, the presence of a second methoxy group, such that methoxy groups occupy both the *meta* and *para* positions, results in a transient capable of undergoing efficient photosolvolysis in the presence of methanol. Studies also show that nucleophilic quenching of the transient is possible by ethanolamine, implicating a stable transient with which a nucleophile can react. Since this compound is not able to form a quinone methide intermediate, the transient for **20** is assigned to the (3,4-dimethoxyphenyl)phenylmethyl cation [eqn. (4)].

Conclusion

The mechanisms of light attenuation by humic substances in aquatic environments are largely unknown. The photoisomerization reactions between catechins **1** and **2** can be described as photon-consuming processes whereby light is absorbed in a repeating, reversible reaction to generate the corresponding isomer. This is an explicit example of a light absorbing reaction that can readily take place in naturally occurring tannin compounds having catechin and epicatechin moieties that may explain in part the mechanism of their sunscreening abilities. Given the relative ease with which the photoisomerization reactions of the simple tannin models can be observed, it may be possible to extend this work to tannin polymers to further explore the photochemistry of these common plant-derived compounds in aqueous environmental systems.

The observed ring-closing mechanism of the *meta*-hydroxybenzhydrol **5** is mainly of theoretical interest as the phenylated derivatives studied here do not represent lignin structures directly, rather they are used as models for the lignin model hydroxybenzyl alcohols that are more difficult to study due to lower reactivity and weaker transient signals. Methoxy-substituted hydroxybenzyl alcohols are important structural elements of the complex and varied molecules that make up the broad group of lignins. The addition of the lignin model methoxy substituent adjacent to the hydroxy group results in quinone methide intermediates that are longer lived than simple mono-hydroxy substituted compounds which has implications

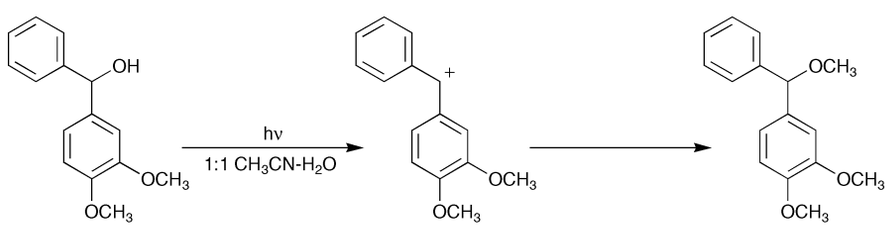

(4)

for lignin degradation and chemistry in aqueous environments. The longer lived the photochemically generated intermediate, the greater the opportunity for reactions to occur that can degrade lignin. Since lignin is a significant proportion of the humic material present in aquatic environments, the photochemistry observed with the model compounds in this study show the types of chemical reactions that can be observed in aqueous environments that can be used to describe lignin transformation processes.

Experimental

General

^{1}H NMR spectra were recorded on either a Bruker AC 300 (300 MHz) or a Bruker 500 (500 MHz) instrument. Chemical shifts are reported in ppm downfield from 0 determined from the residual solvent signal. Mass spectra were analysed on a Kratos Concept IH (EI and HRMS). Melting points were determined by a Reichart 7905 melting point apparatus (uncorrected). UV-Visible spectra and kinetic decays were obtained using a Varian Cary Bio 50 spectrophotometer. Polarimetry measurements were made using a Rudolph Research Autopol III Automatic Polarimeter with a 10 cm cell path length. pH measurements were taken using a Fisher Scientific Accumet Research Dual Channel pH/Ion meter. Preparative thin layer chromatography was performed using 1000 μm silica gel plates from Analtech.

Materials

HPLC grade CH_3CN was distilled over CaH_2 for use in fluorescence measurements. Anhydrous tetrahydrofuran (THF) was obtained by distillation over sodium. 95% ethanol and HPLC grade acetonitrile, dichloromethane, diethyl ether, hexanes, isopropanol, methanol, and toluene were used as received. Mixed solvent proportions are quoted as v:v. PhMgBr in THF for Grignard syntheses was used as received from Aldrich.

(±)-Catechin tetramethyl ether (3). (±)-Catechin (**1**) (7.6 mmol) and $KHCO_3$ (50 mmol) were dissolved in dry acetone (50 mL) under N_2, 2.6 mL dimethyl sulfate was added in increments, and the solution refluxed for 4 h. The cooled suspension was filtered and washed repeatedly with acetone. Several drops of aqueous ammonia were added to the filtrate. Evaporation of the solvent under vacuum yielded an orange solid. Pure product was obtained as a white crystal *via* recrystallisation from methanol (1.81 g, 69%); mp 140.9–144.9 °C; ^{1}H NMR (500 MHz, $CDCl_3$) δ 2.82 (dq, 2H, 4-H), 3.74 (s, 3H, 5-OCH_3), 3.79 (s, 3H, 7-OCH_3), 3.74 (s, 6H, 3′,4′-OCH_3), 4.05 (m, 1H, 3-H), 4.65 (d, 1H, 2-H), 6.09 (d, 1H, 8-H), 6.12 (d, 1H, 6-H), 6.89 (d, 1H, 2′-H), 6.96 (d, 1H, 8′-H) 6.99 (d, 1H, 7′-H); MS (EI) *m*/*z* 330 (M^+); (HRMS) $C_{14}H_{14}O_3$ calc. 330.1467, found 330.1451.

2-Hydroxy-3-methoxybenzhydrol (4). The general procedure for synthesis of **5**, **6**, and **20** followed that described for **4**. A 5.00 g (33 mmol) sample of 2-hydroxy-3-methoxybenzaldehyde was dissolved in dry THF (150 mL) under N_2. PhMgBr in THF (60 mmol) was added dropwise over 15 min and the solution refluxed for 4 h. The cooled reaction mixture was quenched in a mixture of ice and NH_4OAc and brought to pH 10. The THF was removed under vacuum and the remaining aqueous layer acidified with dilute HCl to pH 2, extracted with 4 × 50 mL CH_2Cl_2, dried with $MgSO_4$, and filtered. The CH_2Cl_2 was removed under vacuum to give a yellow oil which was purified twice by column chromatography (CH_2Cl_2) to yield a clear oil that was recrystallised from toluene to yield a white solid (4.66 g, 62%); mp 50.8–54.2 °C; ^{1}H NMR (500 MHz, $CDCl_3$) δ 3.84 (s, 3H, OCH_3), 5.76 (d, 1H, benzyl H), 6.55 (d, 1H, benzyl OH), 6.77–6.81 (m, 2H, ArH), 6.86–6.93 (m, 1H, ArH), 7.20–7.33 (m, 1H, ArH), 7.26–7.30 (m, 2H, ArH), 7.37–7.39 (m, 2H, ArH); MS (EI) *m*/*z* 230 (M^+); (HRMS) $C_{14}H_{14}O_3$ calc. 230.0943, found 230.0945.

3-Hydroxy-4-methoxybenzhydrol (5). The desired product was recrystallised from toluene as white crystals (6.17 g, 82%); mp 99.7–100.9 °C; ^{1}H NMR (500 MHz, $(CD_3)_2CO$) δ 3.78 (s, 3H, OCH_3), 4.62 (d, 1H, benzyl OH), 5.69 (d, 1H, benzyl H), 6.81–6.87 (m, 3H, ArH), 7.16–7.20 (m, 1H, ArH), 7.26–7.3 (m, 2H, ArH), 7.38–7.40 (m, 2H, ArH), 7.42 (s, 1H, ArOH); MS (EI) *m*/*z* 230 (M^+); (HRMS) $C_{14}H_{14}O_3$ calc. 230.0943, found 230.0944.

4-Hydroxy-3-methoxybenzhydrol (6). The desired product was purified twice by column chromatography (CH_2Cl_2) to yield a clear oil which was then recrystallised from toluene to yield a white solid (5.21 g, 69%); mp 89.4–91.4 °C; ^{1}H NMR (500 MHz, $CDCl_3$) 3.84 (s, 3H, OCH_3), 5.54 (s, 1H, ArOH), 5.77 (d, 1H, benzyl H), 6.80–6.82 (dd, 1H, ArH), 6.84–6.86 (d, 1H, ArH), 6.89–6.90 (d, 1H, ArH), 7.23–7.27 (m, 1H, ArH), 7.31–7.34 (m, 2H, ArH), 7.35–7.37 (m, 2H, ArH); MS (EI) *m*/*z* 230 (M^+); (HRMS) $C_{14}H_{14}O_3$ calc. 230.0943, found 230.0937.

3,4-Dimethoxybenzhydrol (20). The desired product was recrystallised from toluene as white crystals (5.64 g, 76%); mp 91.0–93.1 °C; ^{1}H NMR (500 MHz, $CDCl_3$) δ 3.83 (s, 3H, *m*-OCH_3), 3.85 (s, 3H, *p*-OCH_3), 5.78 (s, 1H, benzyl H), 6.81 (d, 1H, ArH), 6.86–6.88 (dd, 1H, ArH), 6.91 (m, 1H, ArH), 7.23–7.27 (m, 1H, ArH), 7.30–7.34 (m, 1H, ArH), 7.35–7.37 (m, 1H, ArH); MS (EI) *m*/*z* 244 (M^+); (HRMS) $C_{14}H_{14}O_3$ calc. 244.1099, found 244.1104.

3-Hydroxy-4-methoxydiphenyl methane (11). A sample of previously synthesized **5** (0.43 mmol) and $NaBH_4$ (5.3 mmol) were added to a quartz photolysis tube and dissolved in 100 mL of 1 : 1 CH_3CN–H_2O. The solution was purged with argon for 15 min, cooled with an internal cold finger to ≤ 15 °C, and irradiated at 254 nm for 20 min. The solution was then acidified to pH 2 with dilute HCl, extracted with 4 × 50 mL CH_2Cl_2, dried over $MgSO_4$ and filtered. The solvent was removed under vacuum. Preparative TLC (CH_2Cl_2, R_f = 0.65) yielded pure product as white crystals in ≈75% yield; ^{1}H NMR (500 MHz, $CDCl_3$) δ 3.85 (s, 3H, OCH_3), 3.89 (s, 2H, benzyl methylene), 5.58 (s, 1H, benzyl OH), 6.67–6.69 (m, 1H, ArH), 6.76–6.78 (t, 2H, ArH), 7.18–7.21 (m, 3H, ArH), 7.26–7.30 (m, 2H, ArH); MS (EI) *m*/*z* 214 (M^+); (HRMS) $C_{14}H_{14}O_2$ calc. 214.0994, found 214.0995.

Product studies

All preparative photolyses were carried out in a Rayonet RPR 100 photochemical reactor equipped with 254 or 300 nm lamps. The solutions were contained in a quartz tube (≈150 mL) which was cooled to ≤ 15 °C with tap water by means of an internal cold finger. All solutions were purged with either argon or nitrogen for a minimum of 10 min before irradiation and for the entire photolysis to facilitate mixing and to maintain an inert atmosphere to minimize photochemical reactions from oxidative reactions. Photolysis times varied from 30 s to 60 min, depending on the system being studied and were run with 16 × 254 nm lamps unless otherwise noted. For photolysis times of ≤ 5 min and for controlled experiments, the lamps were run for 2 min prior to photolysis to ensure a stable output. General work-up of photolysed solutions consisted of neutralization with 0.1 M HCl or NaOH if necessary, addition of 20 mL saturated NaCl followed by extraction with 4 × 50 mL CH_2Cl_2, drying of the organic layer over $MgSO_4$, filtering to remove the drying agent and evaporation of the solvent under vacuum. The irradiation products were separated by preparative TLC and analysed by ^{1}H NMR and MS. In all cases, thermal control experiments were performed under similar conditions of gas

purging and temperature in the absence of light to ensure the contribution of thermal processes to the observed reactivity was insignificant. For pH studies, the pH quoted represents the aqueous layer prior to mixing with CH_3CN.

Photolysis in methanol

The general procedure for photolysis of hydroxybenzhydrols **5**, **6**, and **20** and hydroxybenzyl alcohols **7**, **8**, and **9** followed that described for **4**. A sample of **4** (0.20 mmol) was dissolved in 100 mL of 1 : 1 CH_3OH–H_2O and photolysed for 5 min. Work-up of the products was as described. Preparative TLC separation (CH_2Cl_2) was used to obtain a pure sample of the methyl ether which was identified by ^{1}H NMR (300 MHz, $CDCl_3$) δ 3.45 (s, 3H, benzyl OCH_3), and MS (EI) *m*/*z* 244 (M^+). **5**: δ 3.37; *m*/*z* 244 (M^+). **6**: δ 3.38; *m*/*z* 244 (M^+). **20**: δ 3.37; *m*/*z* 244 (M^+). **7**: δ 3.39; *m*/*z* 168 (M^+). **8**: δ 3.36; *m*/*z* 168 (M^+). **9**: δ 3.35; *m*/*z* 168 (M^+).

Extended photolysis of **5** proceeded as above with 120 mg (0.52 mmol) of sample dissolved in 180 mL solvent. A 20 mL aliquot was subsampled at various intervals and worked-up as described using 4 × 20 mL CH_2Cl_2. Conversion was estimated by ^{1}H NMR integration. The fractions were combined and the individual products separated by preparative TLC (CH_2Cl_2), and analysed by ^{1}H NMR and MS. **10**: benzyl methoxy δ 3.37, *m*/*z* 244 (M^+); **11**: methylene δ 3.87, *m*/*z* 214 (M^+); **12**: aldehyde δ 9.78, *m*/*z* 152 (M^+), and **13**: *m*/*z* 426 (M^+).

Photolysis in acetonitrile

A sample of **2** (0.52 mmol) was dissolved in 1 : 1 CH_3CN–H_2O (150 mL) and photolysed (1 min intervals). A 20 mL aliquot was subsampled at various intervals and worked-up as described using 4 × 20 mL CH_2Cl_2. Conversion of **2** to **1** was estimated from ^{1}H NMR integration of the growth of the catechin (**1**) methylene protons (δ 2.5 ppm) and the decay of the epicatechin (**2**) methylene proton (δ 4.8 ppm).

A solution of **5** (0.22 mmol) was dissolved in 1 : 1 CH_3CN–H_2O (100 mL) and photolysed for 20 min. Preparative TLC (CH_2Cl_2) was used to separate the product mixture. Samples of **17** and the proposed **16** were isolated in trace yields and characterized. Methoxy-substituted hydroxyfluorene (**17**): ^{1}H NMR (500 MHz, $CDCl_3$) δ 3.62 (s, 3H, OCH_3), 3.76 (d, 2H, methylene), 5.43 (s, 1H, OH), 6.36 (m, 1H, methine), 6.41 (m, 1H, methine), 6.53 (d, 1H, methine), 6.71 (d, 1H, methine), 6.92 (m, 1H, methine), 7.08 (m, 1H, methine); MS (EI) *m*/*z* 212 (M^+); Conjugated ketone (**16**): MS (EI) *m*/*z* 212 (M^+).

Quantum yields

Product quantum yields for the photosolvolysis of the methoxy-substituted hydroxybenzhydrol system were determined using relative methods which involved comparison of the yields of photosolvolyzed product between 2-hydroxybenzhydrol with a known quantum yield (secondary actinometric standard) of $\Phi_p = 0.46 \pm 0.03$ [27] and those of the compound in question as determined by ^{1}H NMR integration. A known amount of standard (0.10 mmol) was dissolved in 1 : 1 CH_3OH–H_2O, purged with argon for 10 min, cooled with an internal cold finger to <15 °C, and irradiated for 5 min (254 nm, 4 lamps) to give low conversion (always <30%). An equimolar amount of the compound of unknown quantum yield was irradiated under the same conditions. Products were worked-up as described and isolated by preparative TLC (CH_2Cl_2). Methyl ether products were readily identified by their characteristic ^{1}H NMR methoxy peaks.

Fluorescence spectroscopy

Steady state fluorescence spectra (uncorrected) were taken in a 1 cm² quartz cuvette at 20 °C and recorded on a Photon Technologies International (PTI) QM-2 fluorimeter. Quenching experiments involved the addition of appropriate amounts of H_2O and CH_3CN to give a total volume of 3 mL. The cell was then spiked with the desired compound (in dry CH_3CN for spectra and 1 : 1 CH_3CN–H_2O for quenching experiments) to give an absorbance of ≈0.1 at the excitation wavelength. All solutions were purged with argon for at least 5 min prior to measurement. Fluorescence quantum yields (Φ_f) were calculated by comparing the integrated emission bands of a standard (2-aminopyridine in 0.05 M H_2SO_4 $\Phi_f = 0.60 \pm 0.05$ [35] and 2-hydroxybenzhydrol in aqueous acetonitrile $\Phi_f = 0.13 \pm 0.01$ [27]) with those of the desired compounds. Fluorescence lifetimes (τ_f) were measured on a PTI LS-1 Time-Correlated Single Photon Counting system using an H_2 arc lamp as the excitation source. Software supplied by PTI was used to deconvolute the signals from the lamp and the sample and to fit the decays. All decays were found to be first order.

UV-Visible spectroscopy

Solutions of **4** and **6** with $\Delta OD \approx 0.5$ in a 1 cm² cuvette were prepared from a stock solution in 1 : 1 CH_3CN–H_2O into the desired solvent system using a microsyringe. The solution was purged with argon for at least 5 min, then photolysed for 30 s at 254 nm. The decay spectra were recorded at appropriate intervals to generate a decay trace.

Laser flash photolysis

Transient UV-visible spectra and kinetic measurements were recorded using nanosecond LFP with excitation by a Spectra Physics YAG laser (Model GCR-12; 266 nm excitation, <20 mJ). In a typical flow cell experiment, a solution with $\Delta OD \approx 0.3$ at the excitation wavelength was prepared. The solution was purged with either oxygen or nitrogen for at least 10 min prior to initializing the experiment, and purged continuously throughout. The flow cell system was run at a rate sufficient to provide a fresh solution for each shot from the laser. In a typical static cell experiment for quenching or pH studies, a solution with $\Delta OD \approx 0.3$ at the excitation wavelength was prepared directly in a 7 × 7 mm² quartz cell from a stock solution of the desired compound. Each cell was purged with either oxygen or nitrogen for a minimum of 10 min prior to running an experiment. A millisecond protocol was developed for subsecond experiments that involved manual operation of the detection system. The pulser was disabled, the signal fed directly to the oscilloscope for processing, and the lamp intensity manually offset to detect small transient signals.

Acknowledgements

This research was supported by the Natural Sciences and Engineering Research Council (NSERC) of Canada and the University of Victoria, in particular in the form of a Graduate Fellowship to KF.

References

1 R. Pienitz and W. F. Vincent, Effect of climate change relative to ozone depletion on UV exposure in subarctic lakes, *Nature*, 2000, **404**, 484–487.
2 P. Schmitt-Kopplin, N. Hertkorn, H. R. Schulten and A. Kettrup, Structural changes in a dissolved soil humic acid during photochemical degradation processes under O_2 and N_2 atmosphere, *Environ. Sci. Technol.*, 1998, **32**, 2531–2541.
3 H. Gao and R. G. Zepp, Factors influencing photoreactions of dissolved organic matter in a coastal river of the southeastern United States, *Environ. Sci. Technol.*, 1998, **32**, 2940–2946.
4 R. M. W. Amon and R. Benner, Photochemical and microbial consumption of dissolved organic carbon and dissolved oxygen in the Amazon River system, *Geochim. Cosmochim. Acta*, 1996, **60**, 1783–1792.

5 W. Granéli, M. Lindell, B. M. de Faria and F. de Assis Esteves, Photoproduction of dissolved inorganic carbon in temperate and tropical lakes – dependence on wavelength band and dissolved organic carbon concentration, *Biogeochemistry*, 1998, **43**, 175–195.
6 I. Reche, M. L. Pace and J. J. Cole, Relationship of trophic and chemical conditions to photobleaching of dissolved organic matter in lake ecosystems, *Biogeochemistry*, 1999, **44**, 259–280.
7 C. L. Osburn, D. P. Morris, K. A. Thorn and R. E. Moeller, Chemical and optical changes in freshwater dissolved organic matter exposed to solar radiation, *Biogeochemistry*, 2001, **54**, 251–278.
8 E. Engelhaupt, T. S. Bianchi, R. G. Wetzel and M. A. Tarr, Photochemical transformations and bacterial utilization of high-molecular-weight dissolved organic carbon in a southern Louisiana tidal stream (Bayou Trepagnier), *Biogeochemistry*, 2002, **62**, 39–58.
9 R. G. Zepp, P. F. Schlotzhauer and R. M. Sink, Photosensitized transformations involving electronic energy transfer in natural waters, *Environ. Sci. Technol.*, 1985, **19**, 74–81.
10 G. G. Choudhry, Photophysical and photochemical properties of soil and aquatic humic materials, *Residue Rev.*, 1984, **92**, 59–111.
11 F. H. Frimmel, H. Bauer, J. Putzien, P. Murasecco and A. M. Braun, Laser flash-photolysis of dissolved aquatic humic material and the sensitized production of singlet oxygen, *Environ. Sci. Technol.*, 1987, **21**, 541–545.
12 F. H. Frimmel, Photochemical aspects related to humic substances, *Environ. Int.*, 1994, **20**, 373–385.
13 P. Hapiot, J. Pinson, P. Neta, C. Francesch, F. Mhamdi, C. Rolando and S. Schneider, Mechanism of oxidative coupling of coniferyl alcohol, *Phytochemistry*, 1994, **36**, 1013–1020.
14 I. Kögel-Knabner, The macromolecular organic composition of plant and microbial residues as inputs to soil organic matter, *Soil Biol. Biochem.*, 2002, **34**, 139–162.
15 K. Lorenz, C. M. Preston, S. Raspe, I. K. Morrison and K. H. Feger, Litter decompostion and humus characteristics in Canadian and German spruce ecosystems: Information from tannin analysis and C-13 CPMAS NMR, *Soil Biol. Biochem.*, 2000, **32**, 779–792.
16 C. M. Preston, J. A. Trofymow, B. G. Sayer and J. Niu, ^{13}C nuclear magnetic resonance spectroscopy with cross-polarization and magic-angle spinning investigation of the proximate analysis fractions used to assess litter quality in decomposition studies, *Can. J. Bot.*, 1997, **75**, 1601–1613.
17 C. M. Preston, in *Plant Polyphenols 2: Chemistry, Biology, Pharmacology, Ecology*, ed. G. G. Gross, R. W. Hemingway, T. Yoshida and S. J. Branham, Kluwer Academic, New York, 1999, p. 825.
18 T. E. C. Kraus, Z. Yu, C. M. Preston, R. A. Dahlgren and R. J. Zasoski, Linking chemical reactivity and protein precipitation to structural characteristics of foliar tannins, *J. Chem. Ecol.*, 2003, **29**, 703–730.
19 P. J. Hernes, R. Benner, G. L. Cowie, M. A. Goñi, B. A. Bergamaschi and J. I. Hedges, Tannin diagenesis in mangrove leaves from a tropical estuary: a novel molecular approach, *Geochim. Cosmochim. Acta*, 2001, **65**, 3109–3122.
20 A. C. Stenson, A. G. Marshall and W. T. Cooper, Exact masses and chemical formulas of individual Suwannee River fulvic acids from ultrahigh resolution electrospray ionization Fourier transform ion cyclotron resonance mass spectra, *Anal. Chem.*, 2003, **75**, 1275–1284.
21 W. Bors, W. Heller, C. Michel and M. Saran, Flavonoids as antioxidants – determination of radical-scavenging efficiencies, *Methods Enzymol.*, 1990, **186**, 343–355.
22 D. C. Chu and L. R. Juneja, in *Chemistry and Applications of Green Tea*, ed. T. Yamamoto, L. R. Juneja, D. C. Chu and M. K. Kim, CRC Press, Boca Raton, FL, 1997, p. 13.
23 O. Dangles, G. Fargeix and C. Dufour, Antioxidant properties of anthocyanins and tannins: A mechanistic investigation with catechin and the 3′,4′,7-trihydroxyflavylium ion, *J. Chem. Soc., Perkin Trans. 2*, 2000, 1653–1663.
24 P. G. Pietta, Flavonoids as antioxidants, *J. Nat. Prod.*, 2000, **63**, 1035–1042.
25 C. T. Saucier and A. L. Waterhouse, Synergetic activity of catechin and other antioxidants, *J. Agr. Food Chem.*, 1999, **47**, 4491–4494.
26 P. Wan and B. Chak, Structure reactivity studies and catalytic effects in the photosolvolysis of methoxy-substituted benzyl alcohols, *J. Chem. Soc., Perkin Trans. 2*, 1986, 1751–1756.
27 L. Diao, C. Yang and P. Wan, Quinone methide intermediates from the photolysis of hydroxybenzyl alcohols in aqueous solution, *J. Am. Chem. Soc.*, 1995, **117**, 5369–5370.
28 B. Barker, L. Diao and P. Wan, Intramolecular [4+2] cycloaddition of a photogenerated *o*-quinone methide in aqueous solution, *J. Photochem. Photobiol. A*, 1996, **104**, 91–96.
29 H. C. Longuet-Higgins, Photogenerated quonine methides in aqueous solution, *J. Chem. Phys.*, 1950, **18**, 265.
30 R. C. Weast, *CRC Handbook of Chemistry and Physics*, 62nd edn., CRC Press, Boca Raton, FL, 1981.
31 L. Jurd, Anthocyanidins and related compounds, *Tetrahedron*, 1969, **25**, 2367–2380.
32 I. Vovk, B. Simonovska, P. Vuorela and H. Vuorela, Optimization of separation of catechin and epicatechin on cellulose TLC plates, *J. Planar Chromatogr.*, 2002, **15**, 433–436.
33 D. A. Bolon, *o*-Quinone methides. II. Trapping with production of chromans, *J. Org. Chem.*, 1970, **35**, 3666–3670.
34 A. Arduini, A. Bosi, A. Pochini and R. Ungaro, *o*-quinone methides 2. Stereoselectivity in cycloaddition reactions of *o*-quinone methides with vinyl ethers, *Tetrahedron*, 1985, **41**, 3095–3103.
35 D. F. Eaton, Reference materials for fluorescence measurement, *Pure Appl. Chem.*, 1988, **60**, 1107–1114.
36 C. Cren-Olivé, P. Hapiot, J. Pinson and C. Rolando, Free radical chemistry of flavan-3-ols: Determination of thermodynamic parameters and of kinetic reactivity from short (ns) to long (ms) time scale, *J. Am. Chem. Soc.*, 2002, **124**, 14027–14038.
37 C. Cren-Olivé, S. Lebrun and C. Rolando, An efficient synthesis of the four mono methylated isomers of (+)-catechin including the major metabolites and of some dimethylated and trimethylated analogues through selective protection of the catechol ring, *J. Chem. Soc., Perkin Trans. 1*, 2002, 821–830.
38 S. V. Jovanovic, Y. Hara, S. Steenken and M. G. Simic, Antioxidant potential of gallocatechins – a pulse-radiolysis and laser photolysis study, *J. Am. Chem. Soc.*, 1995, **117**, 9881–9888.
39 D. E. Hathway and J. W. T. Seakins, Autoxidation of catechin, *Nature*, 1955, **176**, 218.
40 P. Kiatgrajai, J. D. Wellons, L. Gollob and J. D. White, Kinetics of epimerization of catechin, *J. Org. Chem.*, 1982, **47**, 2910–2912.
41 W. Peng, A. H. Conner and R. W. Hemingway, Phenolation of (+)-catechin with mineral acids, *J. Wood Chem. Technol.*, 1997, **17**, 341–360.
42 K. Akimoto and I. Sugimoto, Stability of (+)-cyanidanol-3 in aqueous solution, *Chem. Pharm. Bull.*, 1981, **29**, 2005–2011.
43 K. Akimoto, K. Inoue and I. Sugimoto, Photo-stability of several crystal forms of cianidanol, *Chem. Pharm. Bull.*, 1985, **33**, 4050–4053.
44 H. E. Zimmerman and V. R. Sandel, Mechanistic Organic Photochemistry II. Solvolytic Photochemical Reactions, *J. Am. Chem. Soc.*, 1963, **85**, 915–922.
45 R. A. McClelland, V. M. Kanagasabapathy, N. S. Banait and S. Steenken, Flash-photolysis generation and reactivities of triarylmethyl and diarylmethyl cations in aqueous solutions, *J. Am. Chem. Soc.*, 1989, **111**, 3966–3972.
46 R. A. McClelland, N. Mathivanan and S. Steenken, Laser flash-photolysis of 9-fluorenol – production and reactivities of the 9-fluorenol radical cation and the 9-fluorenyl cation, *J. Am. Chem. Soc.*, 1990, **112**, 4857–4861.
47 L. Diao, PhD Thesis, *Photogeneration and chemistry of quinone methides from hydroxybenzyl alcohols*, University of Victoria, 1998.
48 S. L. Murov, I. Carmichael and G. L. Hug, *Handbook of Photochemistry*, Marcel Dekker, New York, 2nd edn., 1993.